Submitted for publication in ApJL
Preprint typeset using LaTeX style emulateapj v. 12/16/11

THE ABUNDANCE OF BULLET-GROUPS IN ΛCDM

J. G. Fernández-Trincado[1,2,3], J. E. Forero-Romero[1], T. Verdugo[3], G. Foex[4] and V. Motta[4]
[1] Departamento de Física, Universidad de los Andes, Cra. 1 No. 18A-10, Edificio Ip, Bogotá, Colombia
[2] Institute Utinam, CNRS UMR6213, Université de Franche-Comté, OSU THETA de Franche-Comté-Bourgogne, Besançon, France
[3] Centro de Investigaciones de Astronomía, AP 264, Mérida 5101-A, Venezuela
[4] Departamento de Física y Astronomía, Universidad de Valparaíso, Avda. Gran Bretaña 1111, Playa Ancha, Valparaíso 2360102, Chile
Submitted for publication in ApJL

ABSTRACT

We estimate the expected distribution of displacements between the two dominant dark matter density peaks and between baryons and dark matter in halos simulated within a full cosmological context. We use as a benchmark the observation of SL2S J08544-0121, which is the lowest mass system observed so far featuring a bi-modal dark matter distribution with a dislocated baryonic component. We extend previous results by studying two halo samples: groups and clusters. We find that 50% to 60% of the dark matter halos with circular velocities in the range $300\,\mathrm{km\ s^{-1}}$ to $700\,\mathrm{km\ s^{-1}}$ (groups) show multimodal morphologies with displacements between the dark matter clumps equal or larger than $133 \pm 21 h^{-1}$kpc as observed in SL2S J08544-0121. For dark matter halos with circular velocities larger than $700\,\mathrm{km\ s^{-1}}$ (clusters) this fraction rises to 80% to 85%. Using the same simulation we estimate the dark matter-to-baryon spatial separation and find that 0.1% to 1.0% of the groups should present separations equal or larger than $87 \pm 14 h^{-1}$kpc corresponding to our observational benchmark; for clusters this fraction is in the range of 4% to 10%, consistent with previous studies of dark matter to baryon separations. The extension of the theoretical predictions and observational results towards low mass Bullet-like configurations, i.e. larger abundance of systems, opens up the possibility for a new statistical test of ΛCDM.

Subject headings: cosmology: theory – dark matter

1. INTRODUCTION

The Bullet Cluster (1E0657—56) provided a new kind of observational evidence for the existence of dark matter (Markevitch et al. 2004; Clowe et al. 2006). Quantifying the displacement between dark matter and the dominant baryonic component (hot X-ray emitting gas) has been used to test the Cold Dark Matter (CDM) paradigm itself by quantifying the substructure velocity required to produce such displacement (Hayashi & White 2006; Springel & Farrar 2007; Thompson & Nagamine 2012), the displacemeent between the dominant dark matter and baryonic component (Forero-Romero et al. 2010) to estimate the expected abundance of such events in a ΛCDM Universe and even explore possible extensions to the concordance cosmological model (Farrar & Rosen 2007; Lee & Komatsu 2010; Lee & Baldi 2012).

Since then, other examples of Bullet-like systems have been found; MACS J0025.4-1222 (Bradač et al. 2008), Abell 2744 (Merten et al. 2011), DLSCL J0916.2+2951 (Dawson et al. 2012), ZwCl 1234.0+02916 (Dahle et al. 2013). Recently (Gastaldello et al. 2014) observed a baryonic-DM displacement if 124 ± 20 kpc in SL2S J08544-0121, a group-like system with a total mass $2.4 \pm 0.6 \times 10^{14}\mathrm{M}_{\odot}$. Systems of this mass are ~ 10 times more abundant than cluster systems in the mass range of the Bullet Cluster $> 10^{15} h^{-1}\mathrm{M}_{\odot}$, this opens up the possibility of observationally finding bullet groups in a fair amount to impose constraints on ΛCDM.

However, a greater abundance of small mass systems has to be weighted by the probability of having a merger and presenting a large displacement between the DM and baryonic components. These two conditions (merger rates, maximum possible displacement) are a funcion of halo mass in ΛCDM cosmologies. Such study has been performed for clusters but not for lower mass systems (Forero-Romero et al. 2010). The existence of objects like SL2S J08544-0121and observational campaigns like the Strong Lensing Legacy Survey (SL2S) open up the possibility of finding multi-modal dark matter distributions in the group mass range.

In this Letter we compute the abundance of group-like dark matter halos with a multi-modal morphology that also might present a DM-baryon displacement. To this end we use a N-body cosmological simulation with such a resolution that allows us to identify multi-modal dark matter distributions in hosts with circular velocities larger than $300\,\mathrm{km\ s^{-1}}$.

This Letter is organized as the follows. In Section 2 we present the simulation and the halo catalogs used in this work. We continue in Section 3 with the geometry of the problem at hand and the measurements setup. Next in Section 4 we present our results and observational perspectives to finally conclude in Sections 6.

2. SIMULATION, HALO CATALOGS AND PAIRS

We use the Bolshoi Run, a cosmological DM only simulation over a cubic volume of $250 h^{-1}$Mpc comoving on a side. The simulation uses the ART code to follow the evolution of a dark matter density field sampled with 2048^3 from $z = 80$ to $z = 0$. The cosmology used corresponds to the spatially flat concordance model with the following parameters: the density parameter for matter (dark matter and baryons) $\Omega_m = 0.27$, the density parameter for baryonic matter $\Omega_b = 0.0469$, the density parameter for dark energy $\Omega_\Lambda = 0.73$, the Hubble parameter $h = 0.7$, the normalization of the Power spectrum $n = 0.95$ and the amplitude of mass density fluctuation (at redshift z=0) $\sigma_8 = 0.82$. These cosmological parameters are consistent with the nine-year Wilikinson Microwave Anisotropy Probe (WMAP) results (Hinshaw et al. 2013). A detailed presentation of the simulation can be found in Klypin et al. (2011).

The number of particles used for each of the DM component was 2048^3, resulting in a mass resolution of 1.35×10^8 $M_\odot h^{-1}$. The completeness limit in this simulation is set for halos with 100 particles corresponding to a mass of $1.35 \times 10^{10} h^{-1} M_\odot$or a maximum circular velocity V_c of 50 km s^{-1}.

We use halo catalogs constructed using the Bound Density Maxima (BDM) algorithm (Klypin & Holtzman 1997; Klypin et al. 1999). To define the radius of a halo we use a density threshold of 360 times the mean density of the Universe, for different redshifts we use the overdensity criterion by Bryan & Norman (1998). An important feature of BDM is that it allows us to detect sub-halos inside larger virialized structures.

All the raw data used in this Letter is available through the Multidark database [1] (Riebe et al. 2013). Furthermore, in order to facilitate the reproducibility and reuse of our results we have made available all the data and the source code available in a public repository [2].

In this Letter we make a study at four different redhifts $z = 0.0, 0.25, 0.5$ and 1.0. First, we select all the host halos (i.e. halos that are not inside a larger halo) with circular velocities $V_c \geq 300$ km s^{-1}. Then, we select the sub-halos with circular velocities $V_c \geq 75$ km s^{-1}. The objective is to use this sub-halos as the tracer of the subdominant dark matter clump in the merging cluster, i.e. the bullets.

For the redshifts $z = 0.0, 0.25, 0.5$ and 1.0 we find 10041, 10346, 10554 and 10382 host halos and 157853, 177331, 195072, 225188 sub-halos, respectively. These two sets (host halos and sub-halos) constitute the basis for our analysis. We find now for each host halo we its most massive sub-halo. Each pair host halo/sub-halo is considered as a potential Bullet system and is kept for the analysis described in the next Section.

3. BULLET GEOMETRY AND MEASUREMENT SETUP

The Bullet-like configurations are composed by two dark matter structures: the host halo and the dominant sub-halo. We describe the kinematics of this configuration by the position and velocity vectors of the sub-halo in a frame of reference where the main halo is at rest; thus $\vec{v} = \vec{v}_{sub} - \vec{v}_{halo}$ and $\vec{r} = \vec{r}_{sub} - \vec{r}_{halo}$, where the subscripts *host* and *sub* refer to the position of the minium of potential for the host and sub-halo in the frame of reference of the simulation, respectively.

The angle between these two vectors can be characterized by,

$$\mu \equiv \cos(\theta) = \frac{\vec{v} \cdot \vec{r}}{||\vec{v}||\,||\vec{r}||}. \quad (1)$$

This encodes relevant information to describe the collision, i.e. cases of $|\mu| \approx 1$ can be considered as head-on collisions while $|\mu| \approx 0$ describes a grazing trajectory.

The geometrical configuration can be further described by the following quantities. The circular velocity of each component, $V_{\rm c,host}$ for the host and $V_{\rm c,sub}$ for the subhalo and the size of the host halo $R_{\rm vir}$. Another useful quantity computed in the simulation is the distance between the minium of potential for the host halo and its center of mass, $X_{\rm off} = ||\vec{r}_{min} - \vec{r}_{cm}||/R_{\rm vir}$ which serves as a measurement of how perturbed is the host halo.

As a zero-th order approximation, in this paper we work with three quantities that are available from observations of Bullet-like systems. The projected distance between two dominant DM clumps, the projected distance between the DM-baryonic clumps and the ratio of the mass associated to the DM clumps.

From the simulation point of view, the first quantity can be translated into the 2D projected values of $||\vec{r}||$ and its value relative to the virial radius $D_{\rm off} = ||\vec{r}||_{\rm 2D}/R_{\rm vir}$. The last quantity, the mass ratio, can be approximated by ratio of the circular velocities of the two clumps $V_{\rm c,sub}/V_{\rm c,host}$ which should be equal to the square root of the mass ratio. The second quantity, the projected DM-baryon distance, is not directly available from a DM-only simulation but, as we show in the Results section, can be inferred from the available information.

In order to gain better insight, we use two quantities that are not readily available from observations but can be measured in the simulation. The first one is the substructure velocity as a fraction of the host's circular velocity, $||\vec{v}||/V_{\rm c,host}$, as a measure of the the strength of the merger. The second is μ to measure the geometry (head-on vs. grazing) of each collision.

The physical quantities described above can be used to describe the three main stages in a bullet-like encounter. First, the sub-halo crosses the virial radius of the host halo starting a head on collision, $||\vec{r}||/R_{\rm vir} \approx 1$ and $\mu \approx< 0.0$. Second, as the sub-halo crosses for the first time the center of the host halo $||\vec{r}||/R_{\rm vir} < 1.0$ and $\mu > 0.0$. Third, as the sub-halo reaches apogee and comes back to the center of the halo $||\vec{r}||/R_{\rm vir} < 1.0$ and $\mu < 0.0$. We use this quantities in the enxt section to fully characterize the different kind of interactions observed in the Bolshoi Run,

4. RESULTS

4.1. *Displacements and Relative Circular Velocities*

The main result of this paper is summarized in Figure 1, it presents the integrated probability distribution for the displacement between the center of the host halo and its dominant sub-halo. The left panel shows the displacement in physical units and the right panel as a fraction of the virial radius of the host halo.

Figure 1 shows the results for two different populations; groups with 300 km s^{-1} $< V_{\rm c,host} <$ 700 km s^{-1} and clusters with $V_{\rm c,host} >$ 700 km s^{-1}. Additionally, this is presented for all redshifts $z = 0.0, 0.25, 0.5$ and 1.0.

The panel with the projected 2D physical displacements also shows a vertical stripe with the estimated displacement for the Bullet-group reported by Gastaldello et al. (2014). In the group sample we see that a fraction of 50% to 60% should present a displacement equal than the estimate for SL2S J08544-0121; in the cluster sample this fraction increases to 80%-85%. This fraction is

[1] www.multidark.org
[2] https://github.com/Fernandez-Trincado/Bullet_Groups-2014

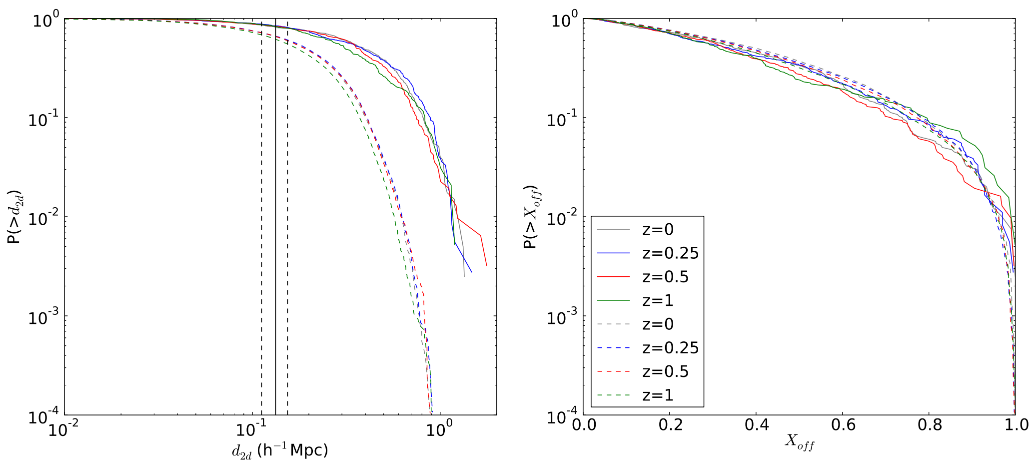

FIG. 1.— Integrated probability distribution for the displacement between the center of the host halo and its dominant sub-halo. The left panel shows the results in terms of the physical displacements while the right panel shows the displacements normalized by the virial radius of the host halo. The continuous (dashed) line corresponds to the halos in the cluster (group). The vertical lines shows the mean and uncertainties in the estimated separation between the two dark matter clumps in the results reported by Gastaldello et al. (2014) for the SL2S J08544-0121. Between 50% to 60% of the groups show a displacement equal or larger than this observational benchmark.

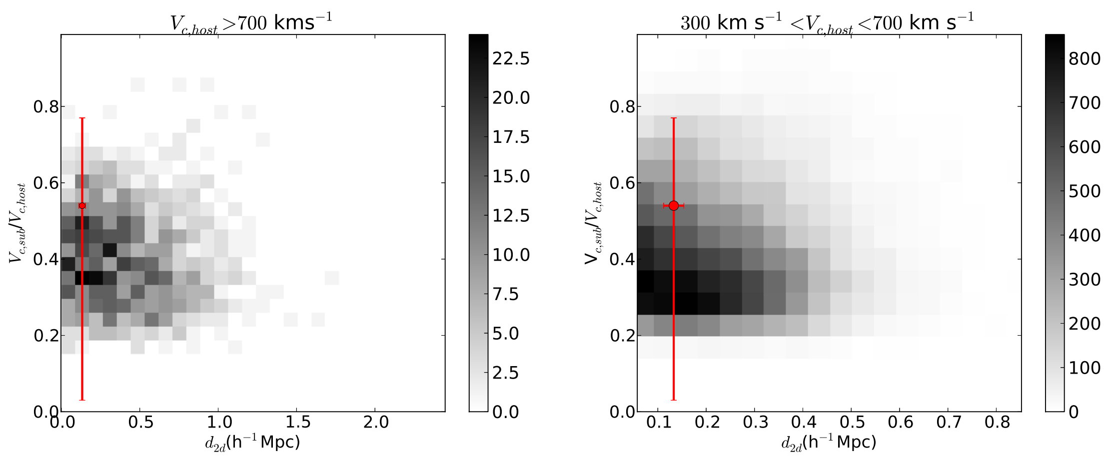

FIG. 2.— 2D histogram in the plane $V_{\rm c,sub}/V_{\rm c,host}$-$d_{2D}$. The left panel corresponds to clusters and the right panel to groups. The star with error bars corresponds to SL2S J08544-0121data reported from Muñoz et al. (2013) and Gastaldello et al. (2014). The data used to construct the histograms integrates the objects at all redshifts.

naturally higher in more massive systems because they are larger in size. Normalizing the displacements by the virial radius, right panel Figure 1, we see that the distribution is the same regardless of the sample and the redshift.

Figure 2 shows 2D histograms in a plane defined by the ratio of the two circular velocities $V_{\rm c,sub}/V_{\rm c,host}$ and the projected 2D physical displacements; quantities that can be constrained by observations. The displacement is a direct observable, while the ratio of the circular velocities can be estimated from lensing studies or approximated by the ratio of the total galaxy luminosity associated with the galaxy peaks or by a lensing reconstruction.

To construct this figure we co-add all the halos in the sample (left, clusters; right, groups) at all redshifts. We stack the data because we do not observe any strong redshift dependence, additionally this allows us to increase the signal in each bin. We overplot a star with error bars that represents the observational estimates for the system SL2S J08544-0121 using the fraction in velocity dispersion in the line-of-sigth of the group SL2S SJ08544-0121 ($\sigma_{host} = 341^{+43}_{-109}$ km s^{-1}and $\sigma_{sub} = 185^{+30}_{-62}$ km s^{-1}) reported by Muñoz et al. (2013) and the DM displacement inferred from the data presented by Gastaldello et al. (2014).

4.2. *Relative Velocities*

In Figure 3 we present the integrated probability of the relative peculiar velocities of the sub-halos with respect to the host halo. The left panel presents this velocity in physical units while the right panel presents them as a fraction of the circular velocity of the host halo.

The panel with the normalized velocities shows that the distribution of sub-halo velocities is close to universal. Regardless of the mass of the host halo and the redshift the integrated distributions lie very close to each

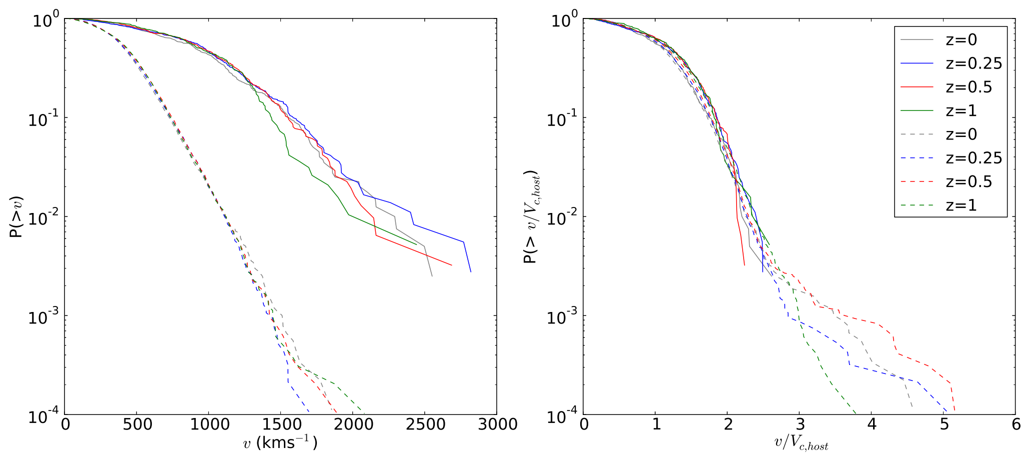

FIG. 3.— Integrated probability distribution for the relative velocity of the sub-halo with respect to its host. The left panel shows the results in physical units while the right panel show the same values normalized by the circular velocity of the host halo. The line encoding follows the same structure as Figure 1

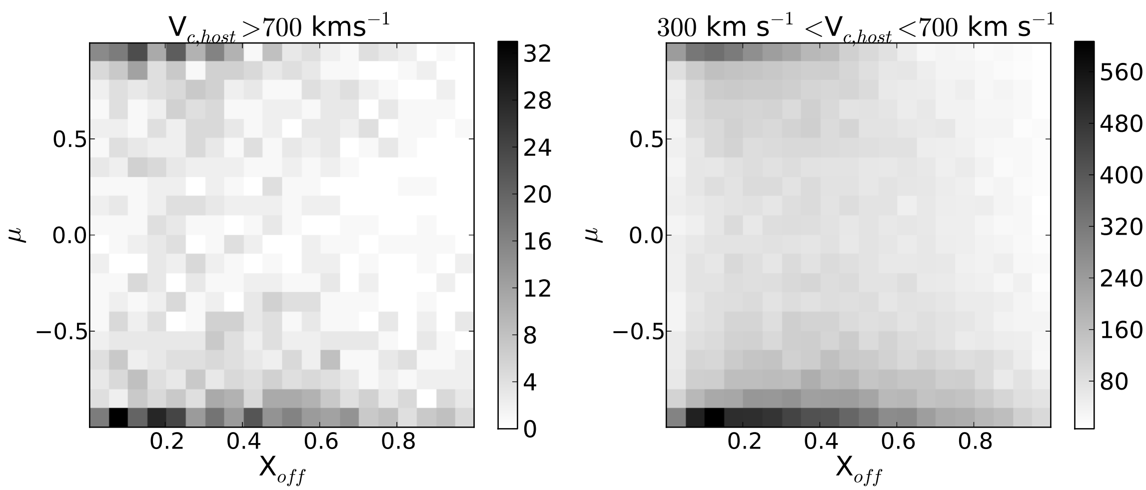

FIG. 4.— 2D histograms in the plane μ-$D_{\rm off}$. The left panel corresponds to clusters and the right panel to groups. The data used to construct this histogram includes the halos at all redshifts.

other. The universality of this profile extends to the group mass range the findings of (Hayashi & White 2006) for clusters.

The median of this distribution is located at $v/V_{\rm c,host} = 1.1$. We also note the strong break at $v/V_{\rm c,host} = 3.0$ that is present in the data from the group sample that allows us to probe fractions on the order of 10^{-4}. This break is located close the escape velocity of $v/V_{\rm c,host}$ for dark matter halos following a NFW profile with a concentration value $c \approx 6$ (Hayashi & White 2006).

4.3. *Collision Geometries*

Figure 4.3 presents the geometry of the bullet groups using the variables μ and $D_{\rm off}$. The first evident feature is that most of the configurations have $|mu| > 0.9$ ($\theta \leq 30°$), meaning that most of the collisions can be described as a head-on encounter while only a minority with $|mu| < 0.9$ have grazing trajectories. For the pairs on radial trajectories there are three regions of interest in this plane that describe different stages in the collision, assuming that the sub-halo merges (or falls below the BDM detection threshold) right at its second pass through the center of the host halo (Poole et al. 2006).

The first region has $\mu \approx -1$ and $D_{\rm off} > 0.6$, which locates the systems where a head-on collision has just started. The sub-halo is close to the boundary of the host halo and is infalling. The second region has $\mu \approx 1$ and $D_{\rm off} < 0.6$; at this stage the collision continues after the first crossing of the host's center, the low number of halos with radial infalling velocities and displacements $D_{\rm off} > 0.6$ suggest that this the maximum range of radii for the apogee. The third region corresponds to $\mu \approx -1$ and $D_{\rm off} < 0.6$ which corresponds to the secondary infall after apogee. We use this sequence in the next subsection to estimate the expected displacement between baryons and the dominant DM clump.

4.4. *Displacement between Dark Matter and Baryons*

Strictly speaking, the results we have derived so far, apply to multi-modal groups and their expected separation between the two dominant dark matter clumps. These displacements cannot be interpreted that all have a corresponding DM-baryon displacement.

However, these different stages for a collision, that we describe at the end of the previous sub-section, can produce different results in terms of the displacement between dark matter and baryons. For instance, the systems where the halo is starting to fall into the host ($\mu \approx -1$, $D_{\rm off} > 0.6$) should not present a detectable DM-baryon displacement. We do expect such displacements when the sub-structure has already passed through the center of the host halo, i.e. cases where $\mu \approx 1$.

In this sub- section we estimate DM-baryon displacement statistics. We work under the following hypothesis. First, we consider that systems with $|\mu| < 0.9$ have a baryonic displacement, $d_{2D}^{\rm bar}$, equal to zero. This means that only head-on encounter produce a displacement. Second, we consider that all systems with infalling velocities $\mu < -0.9$ and large displacements $D_{\rm off} > 0.6$ also have baryonic displacements equal to zero. Third, for all the other cases we estimate the displacement between the baryons and the dominant DM peak by the distances between the dominant peak and the center of mass of the main halo, $d_{2D}^{\rm bar} = X_{\rm off} R_{\rm vir}$, where $X_{\rm off}$ is the offset computed between the minium of potential and the center of mass for each host halo.

This simplified model does not take into account that there is a fraction of halos with $\mu < -0.9$ and $D_{\rm off} < 0.6$ for which the collision has not started and should have $d_{2D}^{\rm bar} = 0$. A detailed modeling of this fraction requires the study of the complete merger tree of the halo and subhalo, a study beyond the scope of this Letter. Instead we caution the reader that the derived fraction of halos with a displacement $< d_{2D}^{\rm bar}$ can be considered as an upper limit.

The results for the integrated distributions for $> d_{2D}^{\rm bar}$ are shown in Figure 5. The dashed lines represented the results for groups and the continuous lines correspond to clusters. As a test of our approach we compare the cluster results against the analytic fit provided by Forero-Romero et al. (2010). This fit reproduces the statistics for the DM-baryon separation found for clusters more massive than $> 10^{14}h^{-1}{\rm M}_{\odot}$in a simulation that included a description for gas with 8 times the volume of the Bolshoi Simulation. The fit is valid for separations larger than $70h^{-1}$kpc , beyond which we find that it provides a remarkably good description within a factor of ~ 2 of our results. This gives us confidence in our approach to estimate the expected fraction of groups with a DM-baryon displacement.

From Figure 5 we see that only a fraction of 0.1% to 1% of the groups are expected to have a DM-baryon displacement equal or larger than $87{\pm}14h^{-1}$kpc as observed in SL2S J08544-0121. This fraction rises to 4% to 10% in the case of clusters, consistent with the results reported by Forero-Romero et al. (2010).

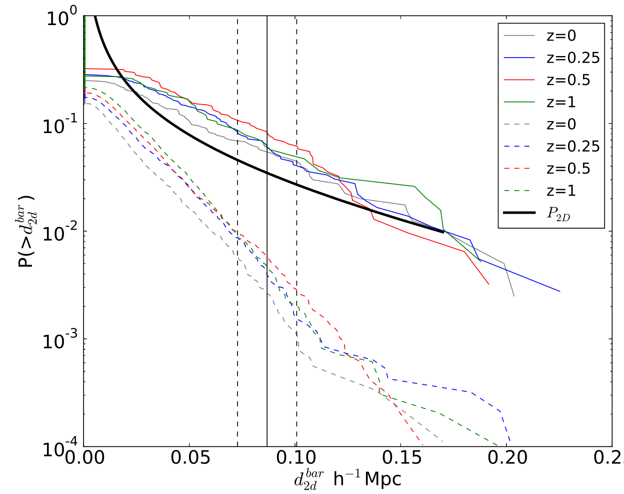

FIG. 5.— Integrated probability distribution for the estimated baryonic displacements in the group and cluster samples. Continous (dashed) lines correspond to clusters (groups). The continuous black line marked as P_{2D} shows the statistics reported by Forero-Romero et al. (2010) for a cosmological simulation including DM and baryons. The vertical lines correspond to the mean value and uncertainty of the displacement measured for SL2S J08544-0121.

5. OBSERVATIONAL IMPLICATIONS

6. CONCLUSIONS

In this Letter we estimate fraction of galaxy groups and clusters that can present observational features associated to a bullet-like event. This is motivated by the recent observational results of (Gastaldello et al. 2014) where a system (SL2S J08544-0121) on the mass range $1 \times 10^{14}h^{-1}{\rm M}_{\odot}$and velocity dispersion 650 km s^{-1}was reported to feature a displacement between its baryonic (hot gas) and dark matter components.

We estimate the distribution of projected displacements between the dominant DM clumps in two kinds of systems; groups with circular velocities $300\,{\rm km\ s}^{-1} < V_{\rm c} < 700\,{\rm km\ s}^{-1}$ and clusters with $V_{\rm c} > 700\,{\rm km\ s}^{-1}$. We report these results at four different redshifts $z = 0.0, 0.25, 0.5$ and 10. Our results based on large N-body dark matter only cosmological simulation with such a resolution that allows to study the group mass range for the first time in the context of Bullet-like configurations.

Our main results is that that a fraction of 50%-60% of the halos in the group sample present displacement equal or larger than the observed displacement for SL2S J08544-0121. For halos in the cluster sample this fraction increases to 80%-85%. We also derive an estimate for the displacement between the DM and the baryonic component. In the group sample 0.1%-1.0% of the halos show a displacement equal or larger than the measurements of SL2S J08544-0121by (Gastaldello et al. 2014). In the cluster sample this fraction rises to 4%-10%.

We also find distributions for the DM separation and the velocity of the bullet through its host. If these quantities are normalized by the virial radius and the circular velocity, respectively, we arrive at distributions close to universal that are similar for the two halo samples at all redshifts.

For the case of SL2S J08544-0121the fair comparison is achieved in the cluster sample, which have statistics dominated by objects of similar mass. In this case we conclude that the existence of such configuration is highly probable in ΛCDM (4% to 10% abundance). In turn, for the same separation the fraction for groups is lower (0.1% to 1%). Taking into account that the difference in spatial abundance between these two samples is on the order of a factor of 10, one can conclude that the absolute number of groups and clusters presenting a DM-baryon displacement larger or equal to SL2S J08544-0121should be of the same order.

However, an interesting observational possibility opens up with surveys such as SL2S that can target a large number of groups and estimate its multi-modal nature from lensing analysis that can be used as a potential test of ΛCDM. In this case the absolute number of groups with a displacement of the same order of SL2S J08544-0121is larger by a factor of ~ 8 than the number of clusters with the same displacement.

The CosmoSim database used in this paper is a service by the Leibniz-Institute for Astrophysics Potsdam (AIP). The BolshoiP simulation was performed within the Bolshoi project of the University of California High-Performance AstroComputing Center (UC-HIPACC) and was run at the NASA Ames Research Center.

REFERENCES

Bradač, M., Allen, S. W., Treu, T., Ebeling, H., Massey, R., Morris, R. G., von der Linden, A., & Applegate, D. 2008, ApJ, 687, 959

Bryan, G. L., & Norman, M. L. 1998, ApJ, 495, 80

Clowe, D., Bradač, M., Gonzalez, A. H., Markevitch, M., Randall, S. W., Jones, C., & Zaritsky, D. 2006, ApJ, 648, L109

Dahle, H., Sarazin, C. L., Lopez, L. A., Kouveliotou, C., Patel, S. K., Rol, E., van der Horst, A. J., Fynbo, J., Wijers, R. A. M. J., Burrows, D. N., Gehrels, N., Grupe, D., Ramirez-Ruiz, E., & Michałowski, M. J. 2013, ApJ, 772, 23

Dawson, W. A., Wittman, D., Jee, M. J., Gee, P., Hughes, J. P., Tyson, J. A., Schmidt, S., Thorman, P., Bradač, M., Miyazaki, S., Lemaux, B., Utsumi, Y., & Margoniner, V. E. 2012, ApJ, 747, L42

Farrar, G. R., & Rosen, R. A. 2007, Physical Review Letters, 98, 171302

Forero-Romero, J. E., Gottlöber, S., & Yepes, G. 2010, ApJ, 725, 598

Gastaldello, F., Limousin, M., & Foex, G. 2014, MNRAS submitted

Hayashi, E., & White, S. D. M. 2006, MNRAS, 370, L38

Hinshaw, G., Larson, D., Komatsu, E., Spergel, D. N., Bennett, C. L., Dunkley, J., Nolta, M. R., Halpern, M., Hill, R. S., Odegard, N., Page, L., Smith, K. M., Weiland, J. L., Gold, B., Jarosik, N., Kogut, A., Limon, M., Meyer, S. S., Tucker, G. S., Wollack, E., & Wright, E. L. 2013, ApJS, 208, 19

Klypin, A., Gottlöber, S., Kravtsov, A. V., & Khokhlov, A. M. 1999, ApJ, 516, 530

Klypin, A., & Holtzman, J. 1997, ArXiv Astrophysics e-prints

Klypin, A. A., Trujillo-Gomez, S., & Primack, J. 2011, ApJ, 740, 102

Lee, J., & Baldi, M. 2012, ApJ, 747, 45

Lee, J., & Komatsu, E. 2010, ApJ, 718, 60

Markevitch, M., Gonzalez, A. H., Clowe, D., Vikhlinin, A., Forman, W., Jones, C., Murray, S., & Tucker, W. 2004, ApJ, 606, 819

Merten, J., Coe, D., Dupke, R., Massey, R., Zitrin, A., Cypriano, E. S., Okabe, N., Frye, B., Braglia, F. G., Jiménez-Teja, Y., Benítez, N., Broadhurst, T., Rhodes, J., Meneghetti, M., Moustakas, L. A., Sodré, Jr., L., Krick, J., & Bregman, J. N. 2011, MNRAS, 417, 333

Muñoz, R. P., Motta, V., Verdugo, T., Garrido, F., Limousin, M., Padilla, N., Foëx, G., Cabanac, R., Gavazzi, R., Barrientos, L. F., & Richard, J. 2013, A&A, 552, A80

Poole, G. B., Fardal, M. A., Babul, A., McCarthy, I. G., Quinn, T., & Wadsley, J. 2006, MNRAS, 373, 881

Riebe, K., Partl, A. M., Enke, H., Forero-Romero, J., Gottlöber, S., Klypin, A., Lemson, G., Prada, F., Primack, J. R., Steinmetz, M., & Turchaninov, V. 2013, Astronomische Nachrichten, 334, 691

Springel, V., & Farrar, G. R. 2007, MNRAS, 380, 911

Thompson, R., & Nagamine, K. 2012, MNRAS, 419, 3560